High-*Q* enhancement of attractive and repulsive optical forces between coupled whispering-gallery-mode resonators

M. L. Povinelli,[1,2] Steven G. Johnson,[3] Marko Lončar,[4] Mihai Ibanescu,[2] Elizabeth J. Smythe,[4] Federico Capasso,[4] J. D. Joannopoulos[2]

[1]*Edward L. Ginzton Laboratory, Stanford University, Stanford, California 94305*
[2]*Department of Physics and the Center for Materials Science and Engineering, Massachusetts Institute of Technology, 77 Massachusetts Avenue, Cambridge, Massachusetts 02139*
[3]*Department of Mathematics, Massachusetts Institute of Technology, 77 Massachusetts Avenue, Cambridge, Massachusetts 02139*
[4]*Division of Engineering and Applied Sciences, Harvard University, Cambridge, Massachusetts 02138*
mpovinel@alum.mit.edu

Abstract: We have calculated the optically-induced force between coupled high-*Q* whispering gallery modes of microsphere resonators. Attractive and repulsive forces are found, depending whether the bi-sphere mode is symmetric or antisymmetric. The magnitude of the force is linearly proportional to the total power in the spheres and consequently linearly enhanced by *Q*. Forces on the order of 100 nN are found for $Q=10^8$, large enough to cause displacements in the range of 1μm when the sphere is attached to a fiber stem with spring constant 0.004 N/m.

©2005 Optical Society of America

OCIS codes: (230.5750) Resonators; (030.4070) Modes; (130.2790) Guided waves; (190.3970) Microparticle nonlinear optics; (290.4020) Mie theory; (999.9999) Optical forces.

References and links

1. W.-P. Huang, "Coupled-mode theory for optical waveguides: an overview," J. Opt. Soc. Am. A **11,** 963-983 (1994).
2. M. L. Povinelli, M. Loncar, M. Ibanescu, E. J. Smythe, S. G. Johnson, F. Capasso, and J. D. Joannopoulos, "Evanescent-wave bonding between microphotonic waveguides," Opt. Lett. (to be published).
3. V. B. Braginsky, M. L. Gorodetsky, and V. S. Ilchenko, "Quality-factor and nonlinear properties of optical whispering-gallery modes," Phys. Lett. A, **137,** 393-397 (1989).
4. L. Collot, V. Lefèvre-Seguin, M. Brune, J.M. Raimond and S. Haroche "Very high Q whispering gallery modes observed on fused silica microspheres," Europhys. Lett. **23,** 327-334 (1993).
5. J. C. Knight, G. Cheung, F. Jacques, and T. A. Birks, "Phase-matched excitation of a whispering-gallery-mode resonances by a fiber taper," Opt. Lett. **22,** 1129-1131 (1997).
6. D. W. Vernooy, V. S. Ilchenko, H. Mabuchi, E. W. Streed, and H. J. Kimble, "High-Q measurements of fused-silica spheres in the near infrared," Opt. Lett. **23,** 247-249 (1998).
7. S. M. Spillane, T. J. Kippenberg, and K. J. Vahala, "Ultralow-threshold Raman laser using a spherical dielectric microcavity," Nature **415,** 621-623 (2002).
8. S. M. Spillane, T. J. Kippenberg, O. J. Painter, and K. J. Valhala, "Ideality in a fiber-taper-coupled microresonator system for application to cavity quantum electrodynamics," Phys. Rev. Lett. **91,** 043902 (2003).
9. V. B. Braginsky, M. L. Gorodetsky, V. S. Ilchenko, and S. P. Vyatchanin, "On the ultimate sensitivity in coordinate measurements," Phys. Lett. A **179,** 244-248 (1993).
10. V. S. Ilchenko, M. L. Gorodetsky, and S. P. Vyatchanin, "Coupling and tunability of whispering-gallery modes: a basis for coordinate meter," Opt. Commun. **107,** 41-48 (1994).
11. H. Miyazaki and Y. Jimba, "Ab initio tight-binding description of morphology-dependent resonance in a bisphere," Phys. Rev. B **62,** 7976-7997 (2000).
12. D. D. Smith, H. Chang, and K. A. Fuller, "Whispering-gallery mode splitting in coupled microresonators," J. Opt. Soc. Am. B **20,** 1967-1974 (2003).
13. J.-P. Laine, B. E. Little, D. R. Lim, H. C. Tapalian, L. C. Kimerling, and H. A. Haus, "Microsphere resonator mode characterization by pedestal anti-resonant reflecting waveguide coupler," IEEE Phot. Tech. Lett. **12,** 1004-1006 (2000).

#8069 - $15.00 USD Received 8 July 2005; revised 23 September 2005; accepted 26 September 2005

14. B. R. Johnson, "Theory of morphology-dependent resonances: shape resonances and width formulas," J. Opt. Soc. Am. A **10,** 343-352 (1993).
15. H. M. Lai, P.T. Leung, K. Young, P. W. Barber, and S. C. Hill, "Time-independent perturbation for leaking electromagnetic modes in open systems with application to resonances in microdroplets," Phys. Rev. A **41,** 5187-5198 (1990).
16. S. Götzinger, O. Benson, and V. Sandoghdar, "Towards controlled coupling between a high-Q whispering gallery mode and a single nanoparticle," Appl. Phys. B **73,** 825-828 (2001).
17. D. R. Rowland and J. D. Love, ''Evanescent wave coupling of whispering gallery modes of a dielectric cylinder,'' Proc. Inst. Electr. Eng. Part J. **140,** 177–188 (1993).
18. M. L. Gorodetsky and V. S. Ilchenko, "Optical microsphere resonators: optimal coupling to high-Q whispering-gallery modes," J. Opt. Soc. Am. B **16,** 147-154 (1999).
19. V. R. Almeida, Q. Xu, C. A. Barrios, and M. Lipson, "Guiding and confining light in void nanostructure," Opt. Lett. **29,** 1209-1211 (2004).
20. J.-P. Laine, H. C. Tapalian, B. E. Little, and H. A. Haus, "Acceleration sensor based on high-Q optical microsphere antiresonant reflecting waveguide coupler," Sensors and Actuators A **93,** 1-7 (2001).
21. T. B. Gabrielson, "Mechanical-thermal noise in micromachined acoustic and vibration sensors," IEEE Trans. on Electron Devices **40,** 903-909 (1993).
22. W. von Klitzing, R. Long, V. S. Ilchenko, J. Hare, and V. Lefèvre-Seguin, "Frequency tuning of the whispering-gallery modes of silica microspheres for cavity quantum electrodynamics and spectroscopy," Opt. Lett. **26,** 166-168 (2001).
23. J. Israelachvili, *Intermolecular and Surface Forces* (Academic Press, London, 1992), Chap. 11.
24. V. P. Mitrofanov, L. G. Prokhorov, and K. V. Tokmakov, "Variation of electric charge on prototype of fused silica test mass of gravitational wave antenna," Phys. Lett. A **300,** 370-374 (2002).
25. J. Ng, C. T. Chan, P. Sheng, and Z. Lin, "Strong optical force induced by morphology-dependent resonances," Opt. Lett. 30, 1956-1958 (2005). An earlier version may be found at URL http://arxiv.org/abs/physics/0502020.
26. M. I. Antonoyiannakis and J. B. Pendry, "Electromagnetic forces in photonic crystals," Phys. Rev. B **60,** 2363-2374 (1999).
27. M. L. Povinelli, M. Ibanescu, S. G. Johnson, and J. D. Joannopoulos, "Slow-light enhancement of radiation pressure in an omnidirectional reflector waveguide," Appl. Phys. Lett. **85,** 1466-1468 (2004).
28. P. T. Leung, S. Y. Liu, S. S. Tong, and K. Young, "Time-independent perturbation theory for quasinormal modes in leaky optical cavities," Phys. Rev. A **49,** 3068-3073 (1994).

Modal splitting arising from coupling between closely-spaced waveguides can be observed in a range of waveguide geometries [1]. Due to overlap of the waveguide fields, symmetric and antisymmetric combinations of the unperturbed modes split in frequency. In a previous paper [2], we have shown that for nanophotonic, high-index-contrast strip waveguides, the attractive and repulsive forces resulting from this splitting are large enough to cause significant displacements. Moreover, the optical force is directly proportional to the optical power in the waveguide modes, suggesting the use of resonant phenomena to further magnify force values.

Whispering gallery mode (WGM) resonances in microspheres are known to have extremely high experimental values of cavity quality factor *Q*, yielding large optical energy enhancements in the microsphere relative to the input power [3–8]. Moreover, modal splitting between coupled microspheres has previously been demonstrated in Refs. [9–12]. For certain choices of the angular mode numbers, a WGM resembles the mode of a curved strip waveguide running around the sphere equator. Efficient methods of coupling to such WGM modes from tapered fiber [8] or integrated waveguides [13] have been experimentally demonstrated and should allow controlled excitation of either symmetric or antisymmetric modes of two-sphere systems. In this paper, we calculate the resulting attractive and repulsive forces between such symmetric and antisymmetric "waveguide-like" modes and show that the optical force is magnified by the cavity *Q*.

A particular WGM is specified by polarization and three mode numbers, the radial mode number *n*, the angular mode number *l*, and the azimuthal mode number *m* [14]. We focus on TE-polarized ($\vec{E}$ perpendicular to the radial direction), fundamental radial modes with $l=m$. The light in such modes is confined not only near the sphere surface, but also near the equator of the sphere. We will consider two microspheres separated by a small gap. Modes of the

#8069 - $15.00 USD Received 8 July 2005; revised 23 September 2005; accepted 26 September 2005
(C) 2005 OSA

bisphere system can be categorized as either antisymmetric or symmetric, as depicted in the inset to Fig. 1.

The force between two weakly-coupled spheres may be calculated from the frequency shift due to coupling [2]. A full derivation is given in the Appendix 1 below. The optical force *F* is:

$$F = -\frac{1}{\omega}\frac{d\omega}{d\xi}U = -\frac{1}{\omega_o + \Delta\omega}\frac{d(\omega_o + \Delta\omega)}{d\xi}U \approx -\frac{1}{\omega_o}\frac{d\Delta\omega}{d\xi}U, \tag{1}$$

where *U* is the total electromagnetic field energy, and ω_o is the unperturbed modal frequency of an isolated sphere. Positive and negative values indicate repulsion and attraction respectively. While the frequency shift $\Delta\omega$ can be directly calculated using vector spherical harmonic expansion [11], such methods become prohibitive for large values of *l*. We employ a perturbative approach, allowing the force to be calculated to first order using only the unperturbed WGM's of the individual spheres. First order results should be sufficient for all data presented here, as the calculated fractional frequency shifts were less than 0.06%. While the modes of a perfect sphere have a *2l*+1 angular degeneracy, slight ellipticities in real, fabricated microspheres remove the degeneracy associated with modes of different *m* [15], with a resulting frequency spacing of many times the linewidth [8, 16]. Nondegenerate perturbation theory thus suffices for practical calculations. Similar perturbative methods have previously been used to calculate modal splitting for waveguide-waveguide [1], waveguide-microsphere [17, 18], and microsphere-microsphere [10] coupling.

The analytical expression for the frequency shift is derived in Appendix 2. The final result is:

$$\frac{\Delta\omega}{\omega_o} = -\frac{1}{2}\frac{\int dV\left[(\varepsilon_2 - 1)\left|E_1^{\,2}\right| + (\varepsilon_1 - 1)\left|E_2^{\,2}\right| \pm \left((\varepsilon_1 - 1)\vec{E}_1^{\,*}\cdot\vec{E}_2 + (\varepsilon_2 - 1)\vec{E}_2^{\,*}\cdot\vec{E}_1\right)\right]}{\int dV\left[\varepsilon_1|E_1|^2 + \varepsilon_2|E_2|^2\right]}, \tag{2}$$

where $\vec{E}_1$ and $\vec{E}_2$ are the unperturbed WGM modes of sphere 1 and sphere 2. The numerator can be separated into two terms, which we will call the *tail:*

$$\int dV\left[(\varepsilon_2 - 1)\left|E_1^{\,2}\right| + (\varepsilon_1 - 1)\left|E_2^{\,2}\right|\right],$$

and the *overlap:*

$$\int dV\left[(\varepsilon_1 - 1)\vec{E}_1^{\,*}\cdot\vec{E}_2 + (\varepsilon_2 - 1)\vec{E}_2^{\,*}\cdot\vec{E}_1\right].$$

The *tail* depends on the integrated power of one sphere's modal profile over the volume of the other sphere. Physically, the resulting frequency shift can be interpreted as a change in the effective path length of the WGM mode of one sphere due to the close proximity of the other sphere (see Ref. [10], which calls this effect the "β-mechanism"). The *overlap* is a "direct" modal coupling term, resulting from overlap of the WGM modes of the two spheres (also known as the "α-mechanism" [10]). We will consider the optical force resulting from the distance dependence of the total frequency shift, incorporating both coupling effects.

The frequency shift $\Delta\omega$ was calculated by numerical evaluation of the modal overlap integrals in Eq. (2). From numerical convergence testing, the finite-grid resolution error (for Cartesian grid spacing of 0.001*a*, where *a* is the sphere radius) is estimated to be less than 4%. Results are shown in Fig. 1 for two sets of angular mode numbers, $l = m = 111$ and $l = m = 184$. The refractive index of the silica microspheres was taken to be 1.47. For these modes, we calculated $x \equiv ka = 2\pi a/\lambda = 80.7466$ and 131.512, respectively. For a wavelength of 1.55 μm, $l = m = 111$ corresponds to a radius of 19.9 μm and $l = m = 184$ to a radius of 32.4 μm.

The optical force between two spheres for either symmetric or antisymmetric modes is shown in Fig. 1. Force is plotted as the dimensionless combination $F\lambda/U$ (left axis) as a

#8069 - $15.00 USD Received 8 July 2005; revised 23 September 2005; accepted 26 September 2005
(C) 2005 OSA

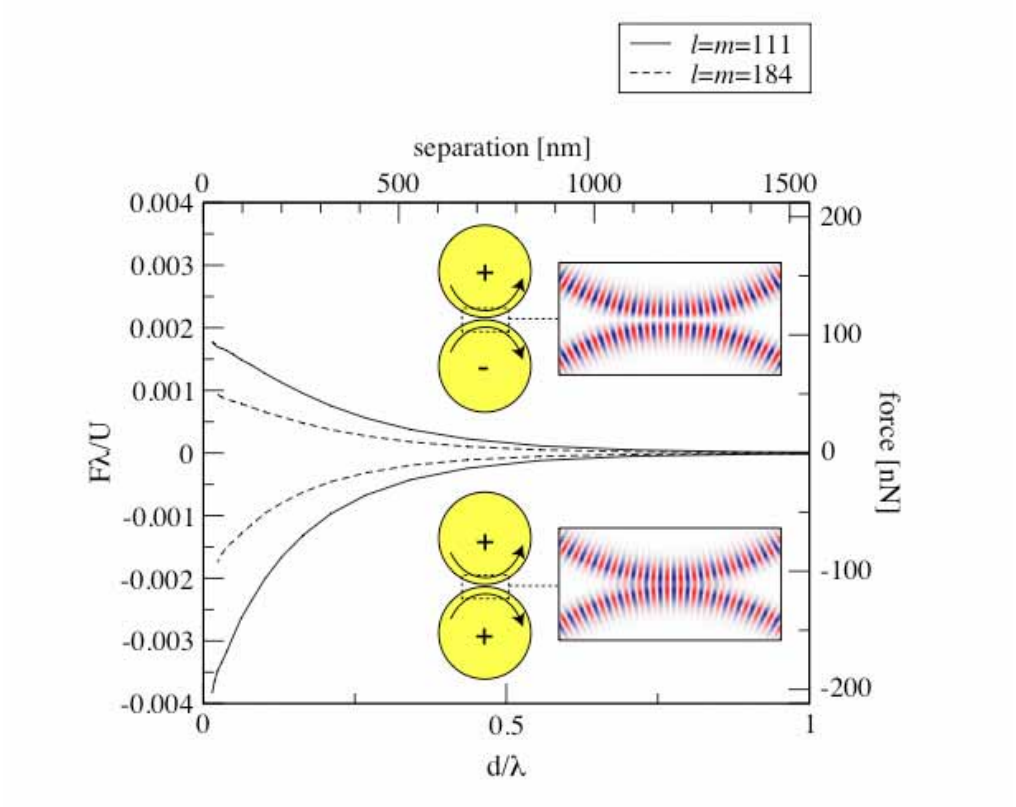

Fig. 1. Force as a function of separation for coupled microspheres for two different angular mode numbers. Negative values indicate attractive forces. Left and bottom axes use dimensionless units. Right and top axes show the force as a function of distance in physical units, assuming a coupled input power of 1mW to each sphere and a Q_o of 10^8. At a wavelength of 1.55 μm, $l = m = 111$ corresponds to a sphere radius (*a)* of 19.9 μm and $l = m = 184$ to a radius of 32.4 μm. Inset shows modal symmetries. For antisymmetric modes (top inset, upper two data curves), the electric field perpendicular to the page points in opposite directions in the two spheres. For symmetric modes (bottom inset, lower two data curves), the opposite is true. Red and blue correspond to electric fields pointing in and out of the page, respectively. Arrows indicate direction of propagation.

function of d/λ (bottom axis), the edge-to-edge separation in units of the wavelength. The symmetric mode of the bi-sphere system gives a negative (attractive) force, while the antisymmetric mode gives a positive (repulsive) force. The trend is the same as for the linear waveguides studied in [2]. It can be seen from Fig. 1 that the values of the attractive and repulsive force are not equal and opposite; the force resulting from the symmetric mode is slightly larger. Comparing force values for the two sets of mode numbers, we see that for fixed d/λ, the magnitude of the force is smaller for the higher mode number. As mode number increases, light is more tightly confined within the sphere, resulting in weaker modal overlap and smaller forces. For all calculations presented in the figure, the force is a monotonically decreasing function of distance. At shorter separations, however, previous work [2] suggests that field-enhancement effects [19] could lead to nonmonotonic behavior.

To calculate the optical force in physical units, we write the total electromagnetic field energy in terms of the coupled input power and cavity quality factor. Under critical coupling conditions [18], the total energy in a single sphere on resonance is $U_1 = P(Q_o/2)/\omega_o$, where *P* is the power coupled into a sphere from an external source and Q_o is the intrinsic quality factor of the resonator. The total energy in the bi-sphere system is then $U \approx 2P(Q_o/2)/\omega_o$. (Small corrections to the total *Q* due to coupling between the two spheres will have negligible

#8069 - $15.00 USD Received 8 July 2005; revised 23 September 2005; accepted 26 September 2005
(C) 2005 OSA

effect on the total energy, since they are higher-order in the modal overlap integrals that determine the frequency shift [18].) Then

$$F = \left(\frac{F\lambda}{U}\right)\frac{U}{\lambda} = \left(\frac{F\lambda}{U}\right)\frac{PQ_o}{\omega_o\lambda} = \left(\frac{F\lambda}{U}\right)\frac{PQ_o}{2\pi c},$$

and the force is directly proportional to PQ_o. Experimental Q_o values greater than 10^8 have been measured for 20-35 μm radius spheres at a wavelength of 1.55 μm [7]. Taking $Q_o = 10^8$ and P = 1 mW, $PQ_o/2\pi c$ = 53 μN. The right and top axes of Fig. 1 show the force as a function of distance in physical units. For sphere separations less than 500 nm, optical forces are in the order of 100 nN. Assuming a lower Q_o of 10^7 or 10^6 will reduce the magnitude of the force by a factor of 10 or 100 accordingly.

To gain intuition for the magnitude of the predicted forces, we calculate the static equilibrium displacements of the spheres. The fabrication process for microspheres involves melting the tip of a silica fiber, leaving the sphere attached to a fiber stem. We consider the case where the two fiber stems are aligned parallel to one another; the optical force between the spheres at their tips will cause the stems to bend. The spring constant of the fiber stem may be written as $k = 3EI/l^3$, where E is the bulk modulus of silica (37 GPa), I is the moment of inertia of the fiber ($I = \pi D^4/64$, where D is the fiber diameter), and l is the length of the fiber stem [20]. For a given k, we can find the equilibrium separation d by setting the spring force $F = -kd/2$ equal and opposite to the separation-dependent optical force. For simplicity, we assume that the power coupled into the spheres is independent of displacement, a reasonable assumption for displacements much less than either the sphere diameter or the fiber length. For fiber lengths l in the range of 5 mm–1 cm and diameters D in the range of 10–125 μm, the spring constant k ranges from $5\text{x}10^{-5}$–10.6 N/m. Clearly, the equilibrium displacement will increase with decreasing spring constant. However, for low enough values of the spring constant, displacements due to thermal fluctuations will become comparable to displacements resulting from the optical force. A conservative estimate of the effect of thermal noise can be obtained by considering a simple measurement of static deflection. Assuming that the measurement is made after any transient motion has died off (e.g. after waiting times greater than the mechanical ringdown time), the thermal displacement can be estimated from the equipartition theorem, $\frac{1}{2}\text{k}_\text{B}T = \frac{1}{2}k\langle x^2\rangle$. The root-mean-square displacement due to fluctuations is then $x_{rms} \equiv \sqrt{\langle x^2\rangle} = \sqrt{\text{k}_\text{B}T/k}$ [21]. We note that spectral analysis of time-dependent displacement measurements can further minimize thermal effects and yield better sensitivity [21], whether under static excitation conditions or, for example, pulsed excitation at the mechanical resonance frequency of the fiber stem.

In Fig. 2, we plot the magnitude of the equilibrium separation d and root-mean-square displacement x_{rms} as a function of spring constant. x_{rms} has been multiplied by 1000 to show both quantities on the same graph. For spring constants $k > 0.004$ N/m, the optically-induced equilibrium separation is greater than 1000 times x_{rms}, and we can safely ignore the effects of thermal noise. The optical displacements in this range are greater than one micron and have equal magnitude for the attractive and repulsive states. For larger spring constants, the attractive state induces a larger displacement, corresponding to larger force magnitudes at smaller separations as shown in Fig. 1. As a numerical example, the choice of length l = 6.0 mm and D = 20 μm (achieved by tapering the fiber stem) gives a spring constant of 0.004 N/m. The equilibrium displacements are 1.16 μm and 0.98 μm for the $n = m$ = 111 and 184 states, respectively. For a larger fiber diameter D = 125 μm and a length l = 1 cm, the spring constant k = 1.33 N/m. For $n = m$ = 111, the equilibrium displacements are 159 nm for the attractive mode and 114 nm for the repulsive mode. For n = m = 184, the displacements are 101 nm and 67 nm, respectively. Equilibrium displacements for other values of Q_oP may

#8069 - $15.00 USD Received 8 July 2005; revised 23 September 2005; accepted 26 September 2005
(C) 2005 OSA

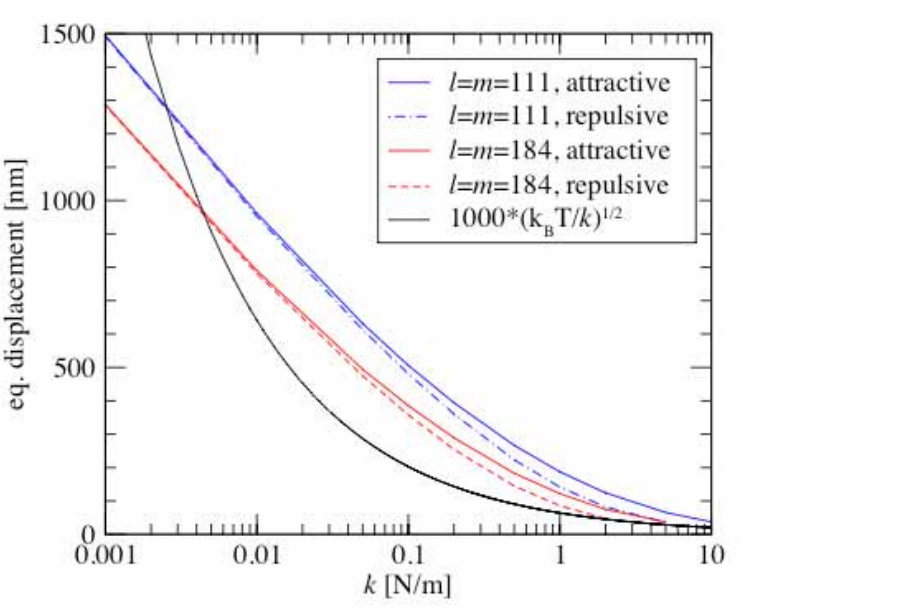

Fig. 2. Magnitude of equilibrium displacement of a sphere due to the optical force as a function of the spring constant k of the attached fiber stem. The optical displacement is larger than 1000 times the estimated thermal displacement (solid black line) for spring constants greater than 0.002 N/m.

easily be deduced from the graph by a simple scaling argument. For a particular k, the equilibrium displacement d is a solution to the equation $F_{opt}(d) = -kd/2$. Reducing Q_oP by a factor α, $F_{opt} \to \alpha F_{opt}$ and d is the solution to the characteristic equation for $k \to k/\alpha$. In other words, a reduction of Q_o to 10^7 will result in the same equilibrium displacement if the spring constant is reduced by a factor of 10.

In the calculations above, we have considered two identical, high-Q spheres. In practice, identical spheres with perfectly coinciding eigenfrequencies cannot be fabricated. As a result, tuning will be required to align resonant frequencies of the two spheres. In Ref. [22], stress-tuning of high-Q (10^9) microsphere resonances by half a free spectral range ($\Delta\nu$ = 400 GHz, corresponding to a ~1% axial strain) was achieved. Fortunately, it should not be necessary to align resonances with *identical* mode numbers to achieve a significant force; l and m may differ between the two spheres. To quantify this claim, we consider the behavior of the tail and overlap integrals (defined following Eq. 2 above) for mismatched l and m. For l = 111, we calculate that a mismatch Δm = 8 ($m_1 = l$, $m_2 = l - 8$) only reduces the integrals by $\leq$80% of their Δm = 0 values. The frequency shift should thus be of the same order of magnitude as for matched spheres. A small mismatch in l between the spheres is also tolerable. For a single sphere, the effect of a small change Δl in the mode number is to slightly increase the radial and angular mode confinement. Consequently, the tail and overlap for modes $l_1 = m_1$ and $l_2 = m_2$ with $l_1 < l_2$ should be no smaller than for two spheres with mode numbers l_2, m_1 and l_2, m_2, and the effect of a l mismatch can be estimated by using the larger l value in the force calculation. As seen from the results of Fig. 1, even a large change in l from 111 to 184 only reduces the force by a factor of order unity; slight l mismatches should preserve the order of magnitude of the optical force. In summary, fabrication differences between the two spheres are not expected to degrade the optical force significantly, provided that two nearby resonances can be tuned to align; both resonances should, however, satisfy the condition that $|m - l| << l$.

#8069 - $15.00 USD Received 8 July 2005; revised 23 September 2005; accepted 26 September 2005
(C) 2005 OSA

In addition to optically-induced forces between the microspheres, Van der Waals forces and electrostatic forces will also be present. The Van der Waals force between the spheres is bounded above by the nonretarded expression $F_{vdw} = Aa/12d^2$ [23], where the value of the Hamaker constant $A \approx 6\times10^{-20}$ J for silica. For a sphere radius a=20 μm and separation of 100 nm, $F_{vdw} \approx 3\,\mathrm{pN}$, roughly four orders of magnitude smaller than the optical force. The electrostatic force arises from stray charges on the silica spheres. Assuming a uniform charge distribution, $F_{es} = kQ_1Q_2/(2a+d)^2$, where Q_1 and Q_2 are the total charges on sphere 1 and 2 respectively, and $k \approx 9.0\times10^9\,\mathrm{Nm^2/C^2}$. For the values of a and d above, $F_{es}/(Q_1Q_2) \approx 5.6\times10^{18}\,\mathrm{N/C^2}$. It is very difficult to predict the total charge values *a priori*, as they are likely to depend sensitively on details of sample preparation and experimental conditions. As a very rough indicator of the expected surface charge, we note that the authors of Ref. [24] measured surface charge densities for a test mass of silica in vacuum ranging from 10^{-14} and 10^{-11} C/cm^2; for our system, such values would result in electrostatic forces ranging anywhere from ~ 10^{-9} to 1 nN. Regardless of their magnitudes, we expect that the electrostatic and Van der Waals forces can easily be distinguished from the optical force due to the linear increase of the optical force with optical power. In addition, both the electrostatic and Van der Waals forces are nonresonant in nature, unlike the optical force.

Subsequent to the submission of this manuscript, similar results were published by Ng *et al* in Ref. [25], which also studies the attractive and repulsive forces between a pair of microspheres resulting from the excitation of morphology-dependent (or whispering-gallery-mode) resonances. Ng *et al* focus on smaller spheres (size parameters kR ~ 28) than those studied here (size parameters kR ~ 80–130). For smaller spheres, direct, numerical calculation of the full, coupled fields of the bisphere system can be employed. The force is then found from numerical integration of the Maxwell stress tensor. For larger spheres, direct calculation becomes increasingly difficult due to the necessity of including higher-order terms in the vector spherical-harmonic expansion. The perturbative formulation we have presented here is particularly suitable in this regime. An additional difference between the work of Ng *et al* and the results presented here is the choice of excitation conditions. Ref. [25] considers excitation of the WGM resonance by an external plane-wave source, while we consider controlled excitation of the individual spheres by e.g. evanescent-wave coupling. Nevertheless, the attainment of qualitatively similar results in different physical regimes and using different methodologies strongly suggests the robustness of the attractive and repulsive optical force phenomenon in coupled-microsphere systems.

Note that like Ref. [25], we also predict the magnitude of the resonant, attractive force to be larger than that of the repulsive force. For symmetric states, the tail and overlap terms in Eq. (2) tend to add together, while for the antisymmetric state, they partially cancel. As the separation between the spheres increases, we observe that the overlap term dominates the tail term, and the forces for the symmetric and antisymmetric states become nearly equal and opposite.

In conclusion, we have shown that large displacements of high-Q silica microspheres result from optical coupling in bi-sphere systems. Along with previous theoretical results on linear waveguides [2, 26] and multilayer films [27], these results suggest an expanding possibility of manipulating the position of integrated optical components using light signals. We are hopeful that experimental observation of such effects will open up a wide range of possibilities for all-optical reconfiguration of integrated-optical devices and nanostructured, artificial materials.

#8069 - $15.00 USD Received 8 July 2005; revised 23 September 2005; accepted 26 September 2005
(C) 2005 OSA

Appendix 1

Here we derive a simple expression for the optically-induced force resulting from coupling of the guided modes of two dielectric objects separated by a distance ξ. A simple argument follows from a quantum "photon" picture, but a more complicated, purely classical proof gives the same result.

Quantum Argument

Consider a closed system of two waveguides separated by a distance ξ. Assume initially that an eigenmode of the full system with frequency ω is excited such that the total electromagnetic field energy is *U*. An adiabatic change in the separation $\Delta\xi$ will shift the eigenmode frequency by an amount $\Delta\omega$. Total energy conservation then implies that the mechanical force on either object is given by

$$F = -\frac{dU}{d\xi} \tag{3}$$

with the convention that positive (negative) values correspond to repulsive (attractive) forces. The field energy may be expressed as $U = N\hbar\omega$, where *N* is the total photon number and $\hbar\omega$ is the energy per photon. Assuming that the photon number is both well-defined in the classical limit and is unchanged by the adiabatic waveguide shift due to the absence of absorption/loss mechanisms,

$$F = -\frac{d(N\hbar\omega)}{d\xi} = -N\hbar\frac{d\omega}{d\xi} = -\frac{1}{\omega}\frac{d\omega}{d\xi}U \tag{4}$$

Classical Argument

Alternately, we can derive the same force expression by expressing the electromagnetic field energy in terms of the eigenmodes of the system for initial separation ξ:

$$U = \frac{1}{4\pi}\frac{1}{2}\mathrm{Re}\left[\int dV\left(\vec{E}_\xi^{\,*}\cdot\vec{D}_\xi + \vec{B}_\xi^{\,*}\cdot\vec{H}_\xi\right)\right] \tag{5}$$

where the (complex) fields are given by a particular solution of Maxwell's equations at frequency ω,

$$\nabla\times\vec{H}_\xi = i\omega\vec{D}_\xi \tag{6}$$

$$\nabla\times\vec{E}_\xi = -i\omega\vec{B}_\xi \tag{7}$$

and may be labeled by (implicit) mode numbers. An adiabatic shift in separation results in a small shift in both the eigenmode frequency and the spatial profiles of the eigenmodes. Applying $\vec{E}_\xi^{\,*}\cdot\partial_\xi$ ($\partial_\xi = \partial/\partial\xi$) to Eq. (6) and $\vec{H}_\xi^{\,*}\cdot\partial_\xi$ to Eq. (7) and subtracting gives

$$\vec{E}_\xi^{\,*}\cdot\left(\nabla\times\partial_\xi\vec{H}_\xi\right) - \vec{H}_\xi^{\,*}\cdot\left(\nabla\times\partial_\xi\vec{E}_\xi\right) = \vec{E}_\xi^{\,*}\cdot\left[i\partial_\xi\omega\vec{D}_\xi + i\omega\partial_\xi\vec{D}_\xi\right] + \vec{H}_\xi^{\,*}\cdot\left[i\partial_\xi\omega\vec{B}_\xi + i\omega\partial_\xi\vec{B}_\xi\right] \tag{8}$$

Integrating the equations over all of space, using the vector identity

$$\vec{b}\cdot(\nabla\times\vec{a}) = \nabla\cdot\left(\vec{a}\times\vec{b}\right) + \vec{a}\cdot\left(\nabla\times\vec{b}\right)$$

and noting that the surface terms vanish gives

$$\omega\partial_\xi\int dV\left(\vec{E}_\xi^{\,*}\cdot\vec{D}_\xi + \vec{B}_\xi^{\,*}\cdot\vec{H}_\xi\right) = i\left(\partial_\xi\omega\right)\int dV\left(\vec{E}_\xi^{\,*}\cdot\vec{D}_\xi + \vec{B}_\xi^{\,*}\cdot\vec{H}_\xi\right) \tag{9}$$

Using Eq. (5), we conclude that

$$\omega\partial_\xi U = U\partial_\xi\omega \tag{10}$$

#8069 - $15.00 USD Received 8 July 2005; revised 23 September 2005; accepted 26 September 2005
(C) 2005 OSA

and the force may be written as

$$F = -\frac{\partial U}{\partial \xi} = -\frac{1}{\omega}\frac{\partial \omega}{\partial \xi}U, \tag{11}$$

in agreement with our previous argument.

We note that for waveguides that are uniform along some (axial) direction, the guided modes of the coupled system can be labeled by a wave number *k*. A shift in separation will preserve translational invariance; as a result, all $\partial/\partial\xi$ derivatives should be taken at fixed *k* as in [2].

Appendix 2

We have derived the frequency shift due to modal splitting from perturbation theory.

For a single, isolated sphere, Maxwell's equations can be recast as a generalized Hermitian eigenproblem:

$$\nabla\times\nabla\times\vec{E}_i - \left(\frac{\omega_i}{c}\right)^2(\varepsilon_i - 1)\vec{E}_i = \left(\frac{\omega_i}{c}\right)^2\vec{E}_i \tag{12}$$

where *i*=1 or 2 labels the sphere and ε_i is the dielectric constant of sphere *i* as a function of position. Defining $\hat{\Theta} \equiv \nabla\times\nabla\times$, $\hat{A}_i = \varepsilon_i - 1$, and $\lambda_i \equiv (\omega_i/c)^2$ and adopting Dirac notation to write $|\psi_i\rangle \equiv \vec{E}_i$, Eq. (12) may be rewritten as

$$\left(\hat{\Theta} - \lambda_i\hat{A}_i\right)|\psi_i\rangle = \lambda_i|\psi_i\rangle \tag{13}$$

For two, non-overlapping spheres, the total dielectric function can be written as $\varepsilon_1 + \varepsilon_2 - 1$, where the constant is subtracted to insure that the dielectric constant is equal to one outside the spheres. Maxwell's equations then become

$$\hat{\Theta}|\psi\rangle - \lambda\left[\hat{A}_1 + \hat{A}_2\right]|\psi\rangle = \lambda|\psi\rangle, \tag{14}$$

where $|\psi\rangle$ is the wavefunction (field) of the total system and λ its eigenvalue. For identical spheres, we can expand the total wavefunction in terms of the single-sphere wavefunctions as $|\psi\rangle = |\psi_1\rangle \pm |\psi_2\rangle + |\psi^{(1)}\rangle + \cdots$, where $|\psi^{(1)}\rangle$ represents a first order correction. Similarly, the eigenvalue can be expanded as $\lambda = \lambda^{(0)} + \lambda^{(1)} + \cdots$. Substituting the expansions into Eq. (14) and making use of Eq. (13), the solution for the zeroth order eigenvalue of the combined system is simply $\lambda^{(0)} = \lambda_1 = \lambda_2$. Left-multiplying Eq. (14) by either $\langle\psi_1|$ or $\langle\psi_2|$ and keeping all first-order terms yields the pair of equations

$$\lambda^{(0)}\left\{\langle\psi_1|\hat{A}_2|\psi_1\rangle \pm \langle\psi_1|\hat{A}_2|\psi_2\rangle + \langle\psi_1|\hat{A}_2|\psi^{(1)}\rangle\right\} + \lambda^{(1)}\langle\psi_1|\left(1+\hat{A}_1\right)|\psi_1\rangle = 0 \tag{15}$$

$$\lambda^{(0)}\left\{\langle\psi_2|\hat{A}_1|\psi_1\rangle \pm \langle\psi_2|\hat{A}_1|\psi_2\rangle + \langle\psi_2|\hat{A}_1|\psi^{(1)}\rangle\right\} \pm \lambda^{(1)}\langle\psi_2|\left(1+\hat{A}_2\right)|\psi_2\rangle = 0 \tag{16}$$

where the inner product is defined as $\langle\psi_i|\psi_j\rangle \equiv \int dV\left(\vec{E}_i^{\,*}\cdot\vec{E}_j\right)$. We can assume that $\langle\psi_1|\hat{A}_2|\psi^{(1)}\rangle << \langle\psi_1|\hat{A}_2|\psi_2\rangle$ since inside sphere 2, the shift $|\psi^{(1)}\rangle$ in the total wavefunction is small compared to the value of the original single-sphere wavefunction $|\psi_2\rangle$. Similarly, for sphere 1, $\langle\psi_2|\hat{A}_1|\psi^{(1)}\rangle << \langle\psi_2|\hat{A}_1|\psi_1\rangle$. Adding Eqs. (15) and (16) and reverting to electromagnetic field notation gives the final expression for the frequency shift,

#8069 - $15.00 USD Received 8 July 2005; revised 23 September 2005; accepted 26 September 2005
(C) 2005 OSA

$$\frac{1}{2}\frac{\lambda^{(1)}}{\lambda^{(0)}} = \frac{\Delta\omega}{\omega_o} = -\frac{1}{2}\frac{\int dV\left[(\varepsilon_2 - 1)\left|E_1{}^2\right| + (\varepsilon_1 - 1)\left|E_2{}^2\right| \pm \left((\varepsilon_1 - 1)\vec{E}_1^{*}\cdot\vec{E}_2 + (\varepsilon_2 - 1)\vec{E}_2^{*}\cdot\vec{E}_1\right)\right]}{\int dV\left[\varepsilon_1\left|E_1\right|^2 + \varepsilon_2\left|E_2\right|^2\right]}. \quad (17)$$

Strictly speaking, the modes of a microsphere resonator are not perfectly confined, and can be described in the near field by a "leaky mode" whose frequency has a small imaginary part [28]. However, for very high-Q modes, the imaginary part of the frequency and the corresponding radiating field pattern far from the spheres can be neglected for our purpose of computing the shift in the real part of the frequency. A parallel derivation to the one above incorporating the modified, leaky-mode overlap integrals of [15] shows explicitly that the corrections to Re[$\Delta\omega$] scale as 1/Q.

Acknowledgments

M. L. P. thanks Stephan Götzinger, Davide Iannuzzi, Mariano Troccoli, Jeremy Munday, Sylvia Smullin, Gabriel Rebeiz, Gabriel Zeltzer, and Brian Lantz for useful discussions. This work was supported in part by the Materials Research Science and Engineering Center program of the National Science Foundation under Award No. DMR-9400334, DoD/ONR MURI Grant No. N00014-01-1-0803, and DARPA contract HR0011-04-1-0032.

#8069 - $15.00 USD Received 8 July 2005; revised 23 September 2005; accepted 26 September 2005
(C) 2005 OSA